

<https://doi.org/10.15407/mineraljournal.44.01.003>
UDC 548.4:552.08

Rainer Thomas, Doctor of Sciences

Helmholtz-Centre Potsdam, German Research Centre for Geosciences
Telegrafenberg, D-14473 Potsdam, Germany

E-mail: RainerThomas@t-online.de; <https://orcid.org/0000-0002-7699-7009>

Paul Davidson, Doctor of Sciences

University of Tasmania, CODES, Centre for Ore Deposits and Earth Sciences
Hobart 7001, Australia

E-mail: Paul.Davidson@utas.edu.au; <https://orcid.org/0000-0002-6129-0748>

Adolf Rericha, PhD. Alemannenstr, 4a, D-14612 Falkensee, Germany

E-mail: ruth.rericha@gmx.de; Scopus ID 6504676937

Dmytro K. Voznyak, Doctor of Sciences

M.P. Semenenko Institute of Geochemistry,
Mineralogy and Ore Formation of the NAS of Ukraine
34, Acad. Palladin Ave., Kyiv, Ukraine, 03142

E-mail: dkvoznyak@ukr.net; <https://orcid.org/0000-0002-6124-2033>

WATER-RICH MELT INCLUSION AS “FROZEN” SAMPLES OF THE SUPERCRITICAL STATE IN GRANITES AND PEGMATITES REVEAL EXTREME ELEMENT ENRICHMENT RESULTING UNDER NON-EQUILIBRIUM CONDITIONS

In this contribution, we show that in miarolitic pegmatites during the crystallization of water-rich melts, samples of these mineral-forming melts were trapped in the form of water-rich melt inclusions, preserved primarily in quartz. The bulk concentration of water and the temperature are the system-determining parameters since from their analysis it follows that these melt inclusions depict pseudo-binary solvus curves in the coordinates of temperature and water concentration. Furthermore, using reduced coordinates (H_2O/H_2O_{crit} vs. T/T_{crit}) most melt inclusions of the studied pegmatites plot very well in a standardized and reduced solvus curve. The existence and formation of such uniform solvus curves is an expression of crystallization processes under nearly equilibrium conditions. However, many trace and some principal elements of the melt inclusions trapped near the solvus crest [H_2O/H_2O_{crit} from 0.5 to 1.5 and $T/T_{crit} > 0.95$] show unusual distributions, with very well-defined Gaussian and/or Lorentzian curves, characterized by defined area, width, offset, and height. This has been shown in many natural examples obtained from pegmatites. Only the offset values represent near-equilibrium conditions and corresponding element concentrations, which are equivalent to the regional Clarke number (Clarke number or Clark is the relative abundance of a chemical element, typically in the Earth's crust). We interpret these distributions as explanation for some extraordinary-chemical properties in this critical region: principally extremely high diffusion rates, low dynamic viscosity and extremely low surface tension. Near the critical point, we have both space and time-related non-equilibrium and equilibrium processes close together. Furthermore, we can show that the Gaussian and Lorentzian distribution are first approximations of the specific element distribution because at the critical point the enrichment of some elements reaches such an extent that the Gaussian and/or Lorentzian curves degenerate into a vertical line (are asymptotic to the concentration axis), which is determined by the maximum solubility of a species in the supercritical melt-water system. The highest concentration of Be, as an example, was observed in Ehrenfriedersdorf melt inclusions: 71490 ppm Be.

Keywords: pegmatites, H_2O -rich melt inclusions, supercritical state, extreme element enrichment, Gaussian/Lorentzian distribution.

Cite: Thomas, R., Davidson, P., Rericha, A. and Voznyak, D.K. (2022), Water-Rich Melt Inclusion as "Frozen" Samples of the Supercritical State in Granites and Pegmatites Reveal Extreme Element Enrichment Resulting Under Non-Equilibrium Conditions. *Mineral. Journ. (Ukraine)*. Vol. 44, No. 1, pp. 03-15. <https://doi.org/10.15407/mineraljournal.44.01.003>

Introduction. At high temperatures melt inclusions in minerals are open systems and represent small aliquots (typical about 10 to 50 μm in diameter) of the molten medium from which the inclusion-bearing crystals grew. After developing a simple Raman-spectroscopic-based method for water determination, in a very large number homogenization experiments under high pressure we have often found extremely water-rich melt inclusions of the type shown in Fig. 1, mostly in pegmatites, however also in granites. Another type of melt inclusion is characterized by salt phases (here mainly NaCl and CaCl_2) in the H_2O -rich liquid phase, as in Fig. 2. In a T-c diagram these inclusions, as a rule, depict a pseudo-binary solvus [14, 26] with an upper critical endpoint (Fig. 3).

This type of diagram is very characteristic for inclusions trapped in crystals (quartz, beryl, topaz) grown under pegmatite-forming conditions at temperatures between 600 $^\circ\text{C}$ and 750 $^\circ\text{C}$ and pressures between about 1 and 5 kbar — mostly in miarolitic pegmatites. However, similar melt

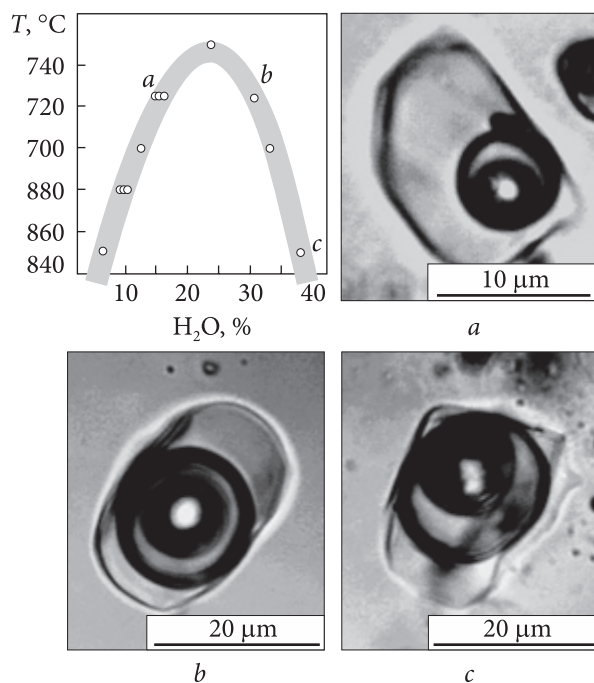


Fig. 1. Melt inclusions in granite quartz (Kirchberg, Saxony). Showing the solvus curve for this granite (top left) and the position of three different melt inclusions (*a*, *b*, and *c*) on this curve. The melt inclusions contain a water-rich glass (about 15, 31, and 38% (g/g) H_2O , respectively) and a water-rich sub-phase (bubble). This type of melt inclusions represents the pre-pegmatitic melts in the intergranular spaces of a granitic rock

inclusions can be found in other pegmatites and even in evolved granites, often arranged in approximately vertical channels which served as conduits for pegmatites or embryonic hydrothermal veins. The water-rich melt inclusions in minerals, mostly quartz and topaz, of some granitic rocks form similar pseudo-binary solvi in the coordinates H_2O -T (see Fig. 4). The deviations from the ideal solvus curve are, in contrast to pegmatites, significantly larger, because during the melt moving along the channels the melt is in a steady-state with the changing environment. We can call this type of melt inclusions "pre-pegmatitic" because the composition is very water-rich but highly variable. Collecting a larger number of different fractions in a single miarolitic cavity result in the formation of a "standard" pegmatite-forming melt.

At this point it is important to note that the water contents in the silicate melt discussed in this paper are extremely high, and quite contrary to the bulk "haplo-granitic systems" with water concentrations <8%. To maintain a water content of about 30% in such a simple system, a pressure of about 20 kbar is necessary. However, such high pressures are unrealistic for normal pegmatites (typically <5 kbar) and granites. That means, for such high water contents in a pegmatite-forming melt we need high alkali concentrations [2] or B_2O_3 or F_2O_{-1} in excess [11] in their composition. This holds true also for the pre-pegmatite melts.

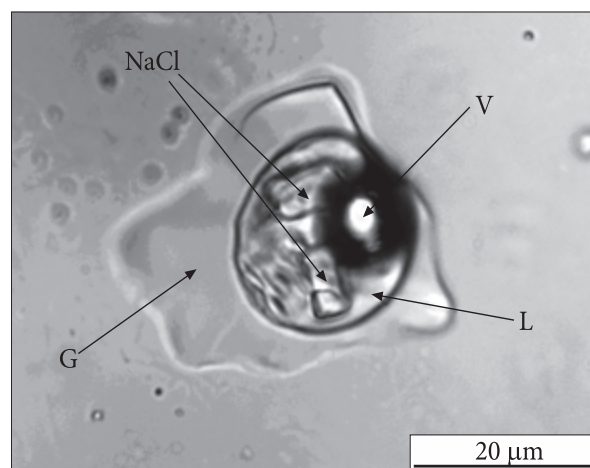


Fig. 2. Type-A melt inclusion in quartz from Steinitz-wolmsdorf/Lusatia. This inclusion contains glass (G), a liquid H_2O -rich phase (L), and a vapor phase (V). In the liquid phase there are crystals of NaCl and also CaCl_2

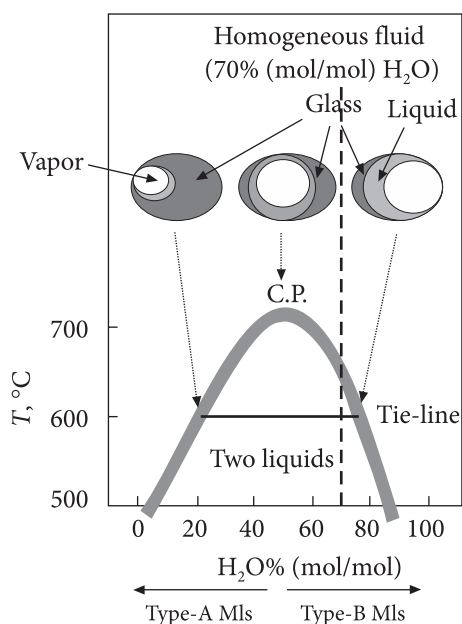


Fig. 3. Schematic characteristics of three different melt inclusion types (type-A, near-critical, and type-B) in pegmatitic minerals, mostly quartz, topaz, and beryl, at room temperature after re-homogenization at given temperatures and pressures between 1 and 5 kbar. The arrows show the relations of the melt inclusions to the solvus of the pseudobinary melt- H_2O -system. C.P. — critical point [24]

Another remark is important, in more than 650 homogenization and quenching experiments under pressure we have never observed a gel-like state in the quenched inclusions, neither in pegmatites nor in granites. All silicate-rich phases formed metastable glasses, some of which dissociated into two or more phases after some time had elapsed.

Fig. 5 show the results after re-homogenization under pressure, and the water determination for inclusions in pegmatites in the form of a solvus diagram in reduced coordinates $H_2O/H_{2O_{crit}}$ vs. T/T_{crit} derived from several different pegmatites. The similarity of the solvus curves of such complicated systems as pegmatites was at first surprising. At and near the solvus crest some elements (Be, B, F, Na, P) are enriched in the corresponding melt inclusions to a significantly higher level than in the bulk rock (mostly granites). The second surprise was the finding that some, commonly extremely rare elements, such as Be, follow a regular pattern in the form of a Gaussian or Lorentzian distribution around the critical point of the corresponding solvus. The strong element distribution around the critical

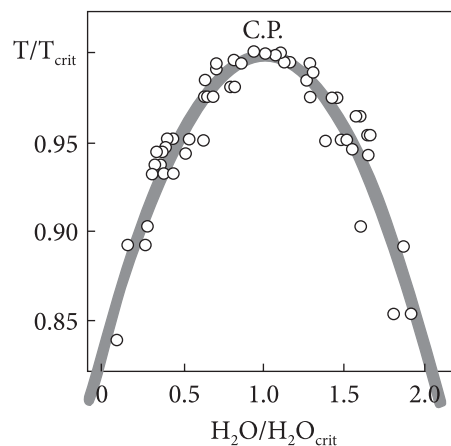


Fig. 4. The pseudo-binary solvus curves for different granites. T_{crit} is the critical temperature; H_2O_{crit} is the water concentration at the critical point. Note: each point represents the mean of measurements on up to 100 melt inclusions [22]. C.P. — critical point

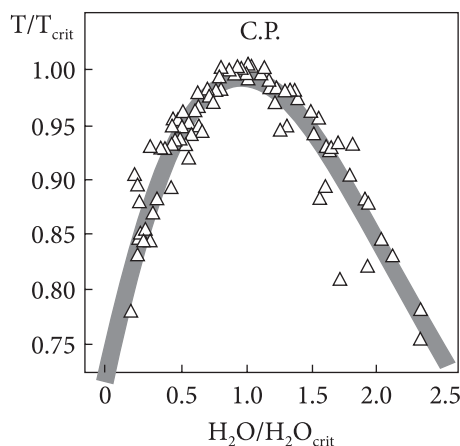


Fig. 5. The pseudo-binary solvus curves for different pegmatites using normalized temperature and water concentration. Values have been normalized to the critical temperature (T_c) as well as the critical water concentration for each system; therefore, the data from different systems can be shown on the same plot (simplified after [19]). C.P. — critical point

point looks like the "derby-hat" region discussed by Harrison and Mayer [3]. The offset of these curves represents the "normal" enrichment of these elements in pegmatites and Gaussian and/or Lorentzian distributed extremely enriched elements follows a previously unknown principle. The highly selective enrichment of some elements is surprising and cannot be explained only by equilibrium processes.

The high solubility of a species alone is not sufficient to explain such high concentrations — we need a highly selective and effective enrichment process to reach such concentrations in the

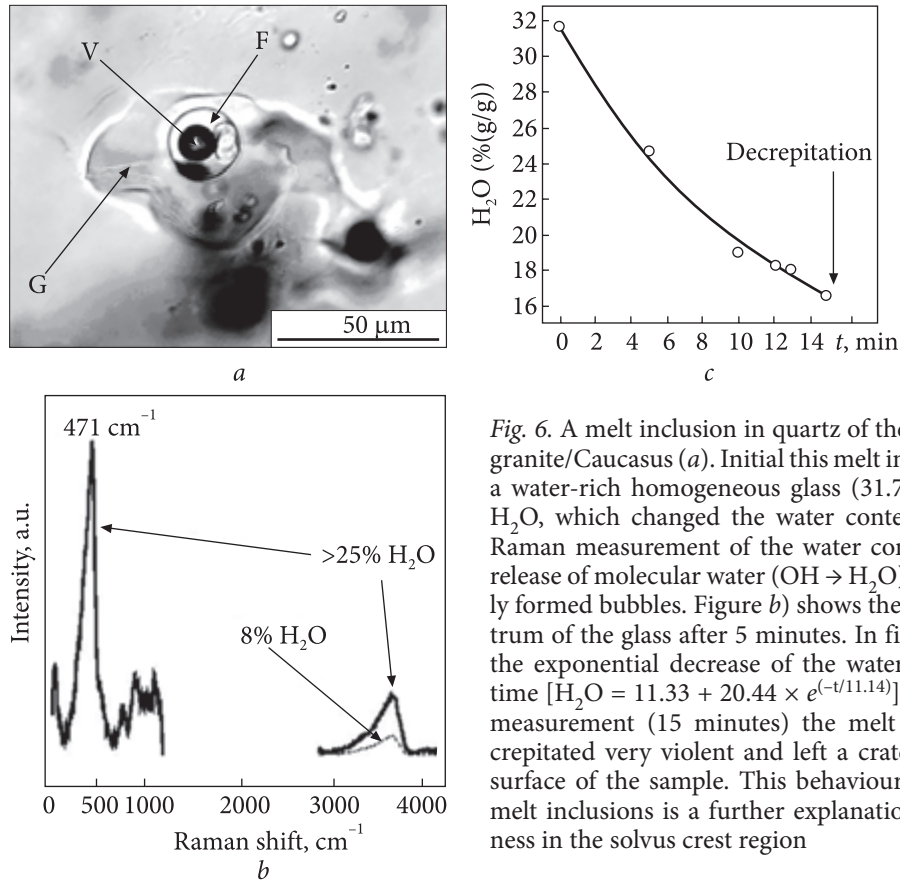


Fig. 6. A melt inclusion in quartz of the Eldzhurtinsk granite/Caucasus (a). Initial this melt inclusion shows a water-rich homogeneous glass ($31.7 \pm 2.4\%$ (g/g) H_2O), which changed the water content during the Raman measurement of the water concentration by release of molecular water ($\text{OH} \rightarrow \text{H}_2\text{O}$) into the newly formed bubbles. Figure (b) shows the Raman spectrum of the glass after 5 minutes. In figure (c) is seen the exponential decrease of the water content with time [$\text{H}_2\text{O} = 11.33 + 20.44 \times e^{(-t/11.14)}$]. After the last measurement (15 minutes) the melt inclusion decrepitated very violent and left a crater in the back surface of the sample. This behaviour of water-rich melt inclusions is a further explanation for the flatness in the solvus crest region

first place. Currently, such processes are unknown and are in all probability strongly disequilibrium processes. There is a "molecular communication" possibly of the type "molecule correlation" generated in the supercritical state. It is important to note that water alone is not a sufficient explanation. Small changes around the critical point lead to a reversal of the sign. Starting at the critical point we observe two approximately equal symmetric branches which open with cooling to the left side (type A-melt) and to the right side (type B-melt). Immediately at the critical point (with the highest concentration), we observe therefore a depletion to the left side of the C.P. and a depletion the right side of the C.P., which suggests two nearly anti-symmetric complex exponential functions.

In this contribution, we will only present the most important results for understanding the extreme element enrichment connected with crystallization processes near the critical point (critical range). The results should serve as a basis for more detailed and theoretical considerations in future. The geological background, the methodology for determining the solvus curves,

and the corresponding element distribution are given in several previous contributions [14, 15, 17-19, 20, 23, 26, 27].

Results. Given their characteristic occurrence (phenotype of near-critical melt inclusion) the study of extremely water-rich melt inclusions after partial homogenization under pressure is relatively simple because these inclusions are visually distinct (see Fig. 1). The figure shows the appearance of melt inclusions trapped at the pseudo-binary solvus curve.

This phenotype is characterized by three phases: vapor bubble ($\sim 20\%$ (vol/vol)), fluid-phase ($\sim 32\%$ (vol/vol)), and a water-rich glass ($\sim 48\%$ (vol/vol)). Dependent on the temperature, water concentration, and cooling rate, these phase relations vary within wide limits. It is important to note that immediately after homogenization and only with very rapid quenching ($100\text{ }^\circ\text{C/s}$), using the hydrothermal rapid-quench homogenization technique, this type of inclusion forms a homogeneous, but typically metastable glass, which after a short time at room-temperature, dissociates by relaxation into the three described stable phases: water-bearing glass, fluid, and a vapor bubble.

Fig. 6 shows an example of the decrease of the water content of an initial homogeneous glass with time during Raman measurements. The energy of the laser light accelerates the spontaneous disintegration of the homogeneous glass into homogeneous glasses with lower water content and the formation of an increasing bubble that acquires the liberated water. The water content of the quenched glass generally corresponds to the pressure used for the homogenization. Sometimes there are also mineral phases, as for example crystals of sassolite, topaz, and alkali carbonates may be present. Using the standard cold-seal pressure vessel homogenization technique with a quenching rate of about 2°C/s the conservation of the homogeneous bulk phase (melt/glass) is generally not possible, given the low quenching rate the separation into glass-, liquid- and vapor components cannot be prevented.

This at least implies that a steady-state situation is formed by the quenching, depending on the real cooling rate, pressure, and on the composition. An important limitation here is that the analytical study of one phase does not represent the whole system. Since the physical properties of glass, liquid and vapor require different techniques, and some homogenization and cooling induced changes may be irreversible. At best, if the study of both main phases (with different methods) is possible, we obtain a first approximation for the system. The complete description of the system is in principle not possible, since we are viewing only a small aliquot separated in time and physical conditions from the original system. It is furthermore very important that the reference feature used (H₂O), mostly the liquid water, can be determined with adequate accuracy. This reference standard for comparison is significant in our view.

The results of the extreme enrichment of some elements are summarized in Table. There are given for different ions (from different localities) along with the data for the corresponding Lorentzian and Gaussian distributions (area A, centre, width, offset, height H, and the ratio A/H).

As examples, we will discuss the extreme Be-enrichment in the Ehrenfriedersdorf pegmatite, which was the first example noted of a Gaussian element distribution, as well as the fluorine enrichment in melt inclusions in quartz of a Volyn chamber pegmatite.

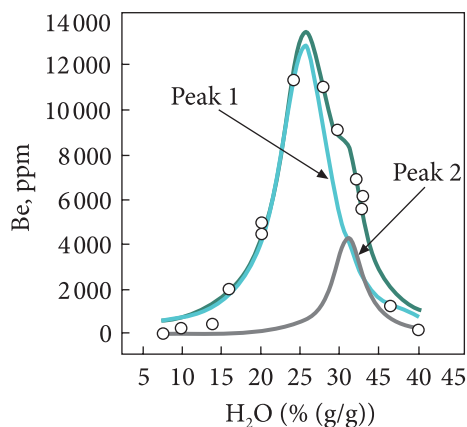


Fig. 7. Distribution of Be in some melt inclusions in pegmatite quartz from Ehrenfriedersdorf. The sum curve result from the overlapping of two Lorentzian components caused by different Be-species in the melt inclusions: Peak 1 for beryllonite [NaBePO₄], and peak 2 for hambergite [Be₂BO₃(OH,F)]. Peak 1 (centre 25.5% (g/g) H₂O, width 7.5% (g/g) water, height 12 840 ppm Be). Peak 2 (centre 31.0% (g/g) H₂O, width 4.8% (g/g) H₂O, height 4280 ppm Be)

Beryllium enrichment in melt inclusions in quartz of the Ehrenfriedersdorf pegmatite. In Thomas et al. [25] it could be shown for the first time that the rare element Be can be enriched to extremely high values of 10,000 ppm or more in the H₂O-rich melt fractions of the Ehrenfriedersdorf granite-pegmatite system. Correlating the Be concentration with the water concentration of the corresponding melt inclusions obtains an excellent Gaussian distribution of Be versus H₂O [16]. The corresponding data are given in Table. Fig. 7 shows a composed Lorentz fit for several Be-rich melt inclusions in the Ehrenfriedersdorf pegmatite quartz. The two Lorentzian components are the result of different Be-phases in the inclusions: Beryllonite [NaBePO₄] vs. hambergite [Be₂BO₃(OH,F)].

Far higher enrichments for Be were observed for hambergite-rich melt inclusions in morganite crystals from the Muiane pegmatite, Mozambique. Here we have measured 37.8 (% (vol/vol)) BeO in synthetic melt inclusions generated at 650°C, corresponding to about 490,000 ppm BeO (or 176,556.8 ppm Be) — [13].

Subsequently, a larger number of such Gaussian or Lorentzian distributions of different elements or molecules versus the water concentration were found in very different pegmatites and granites (see Table). However, a concise discus-

Element enrichment near the solvus crest and data of the corresponding Lorentzian and Gaussian functions of the studied ions

No.	Origin	Ion	Radius, Å	Charge	Area	Center H ₂ O% (g/g)	Width H ₂ O% (g/g)	Offset, ppm	Height, ppm	A/H	<i>n</i>
1	E-Dorf	BO ₃	2.68	3-	153 500	25.5	7.67	0	12 730	12.06	23
2-G	E-Dorf	Be	0.34	2+	131 560	26.0	8.88	284	11 810	11.14	14
3	E-Dorf	Be	0.34	2+	32 261	32.0	4.97	0	4 133	7.80	110
4	E-Dorf	As	0.58	3+	46 433	30.2	3.19	521	9 266	5.01	20
5	E-Dorf	Ta	0.68	5+	50 148	27.4	9.87	86	3 236	15.50	18
6	E-Dorf	Zn	0.83	2+	208 400	27.0	5.78	-754	22 950	9.08	9
7	E-Dorf	Sn	1.12	2+	54 207	25.8	5.22	547	6 606	8.21	46
8	E-Dorf	Cs	1.65	1+	266 000	26.0	5.63	1 300	30 000	8.87	18
9	E-Dorf	Cl	1.81	1-	147 040	27.2	4.98	902	18 782	7.83	63
10	E-Dorf	PO ₄	3.00	3-	1 331 000	28.5	7.49	1300	113 100	11.76	29
11	E-Dorf	WO ₄	3.52	2-	73 258	26.6	7.41	303	6 292	11.64	7
12	Zinnwald	F	1.33	1-	104 590	28.7	4.73	43 671	14 063	7.44	8
13	Zinnwald	Rb	1.49	1+	50 926	23.9	2.95	4 267	13 791	3.69	18
14	Zinnwald	Cs	1.65	1+	100 510	27.1	2.08	118	30 719	3.20	39
15	Königshain	SiO ₄	2.23	4-	2 166 000	30.0	6.77	10 300	203 700	10.63	7
16-G	Königshain	SiO ₄	2.23	4-	1 413 000	30.0	6.77	6 698	132 902	10.63	10
17	Oppach	Na	0.98	1+	3 215 500	27.7	6.10	22 413	335 670	9.58	10
18	Oppach	SO ₄	2.36	2-	1 751 000	27.7	6.10	12 206	182 800	9.58	25
19	Oppach	Be	0.34	2+	164 270	27.7	6.10	1 145	17 148	9.58	10
20	Steinigtwolmsdorf	Na	0.98	1+	2 587 000	29.8	6.59	16 800	250 000	10.35	8
21	Steinigtwolmsdorf	Ca	1.06	2+	541 000	32.0	7.45	1 100	57 900	9.34	5
22	Steinigtwolmsdorf	OH	1.53	1-	1 269 000	30.0	5.70	24 000	141 900	8.94	8
23	Steinigtwolmsdorf	Cl	1.81	1-	240 900	29.8	6.59	15 600	23 300	10.34	63
24	Habachtal	Mg	0.78	2+	165 840	28.8	5.28	4 547	19 974	8.30	10
25	Habachtal	CO ₃	1.85	2-	409 920	27.5	5.28	11 239	49 371	8.30	10
26	Huber-Stock	WO ₄	3.52	2-	880 060	29.7	8.73	2 915	80 454	10.94	9
27	Elba	Li	0.78	1+	288 300	30.0	6.78	1 358	27 085	10.64	7
28	Elba	Cs	1.65	1+	558 270	30.0	6.78	2 630	52 445	10.64	7
29	Tyrnyauzsk	Fe	0.83	2+	487 350	29.2	8.37	1 000	46 438	10.49	6
30	Orlovka	Be	0.34	2+	268 000	29.6	6.61	1 476	25 776	10.40	10
31	Orlovka	CO ₃	1.85	2-	3 565 900	29.6	6.61	19 661	343 270	10.40	10
32-G	Volyn	F	1.33	1-	45 090	20.380	8.1559	0	44 111	10.22	11
33-G	Volyn	F	1.33	1-	72 261	30.276	8.1185	0	71 019	10.18	11

Note. The data for the Lorentzian and Gaussian functions are from [19] and this work. Important are the area, the height and the ratio between area and height (A/H). For two overlaying Lorentzian element distributions is the offset 0. The "G" at the No. means, that this ion is Gaussian distributed. *n* — number of analyses. The data for the ion radii are from [1]. *Explanatory notes to the origin of the studied quartz samples: E-Dorf:* Chamber pegmatite in the tin-tungsten deposit Ehrenfriedersdorf, Erzgebirge/Germany. *Zinnwald:* F-rich topaz-albite granite from Zinnwald, E-Erzgebirge/Germany. *Königshain:* Mirolitic pegmatites in the granite from Königshain/Lusatia, E-Germany. *Oppach:* Quartz-specularite vein in an aplite vein in granodiorite, Lusatia, E-Germany. *Steinigtwolmsdorf:* Quartz vein in granodiorite, Lusatia, E-Germany [22]. *Habachtal:* Melt inclusions in emerald from the Habachtal/Austria. *Huber-stock:* Horni Slavkov, Sn-W ore district, Bohemian Massif, Czech Republic (evolved topaz-albite granite). *Elba:* Marolitic pegmatite in Elba granite, Island of Elba, Italy. *Tyrnyauzsk:* Granite from Eldzhurtinsk, Caucasus, Russia. *Orlovka:* Orlovka amazonite granite, East Transbaikalia, Russia. *Volyn:* Chamber pegmatite from Volodarsk-Volynski, Ukraine.

sion of the results presented in this table remains for a separate manuscript.

A general note: such extreme element enrichments cannot be explained by a simple classical equilibrium processes, because this enrichment is produced by many fundamental steps, which are currently unknown in detail. To these steps belong the selective enrichment and simultaneously movement of a specific ion into the supercritical trap. That means that a dispersed low concentrated specific ion in a practical infinite volume will be concentrated at or near the critical region in an exponential manner. Thus, in a large volume separated specific ion move into the direction of the supercritical state with a higher rate than other elements.

Fluorine enrichment in melt inclusions in quartz from a Volyn chamber pegmatite. After homogenization, Raman-spectroscopic water determination and volume measurements on melt inclusions in quartz crystals from a Volyn chamber pegmatite [28] we have obtained a pseudo-binary solvus curve in the coordinates water concentration vs. temperature (Fig. 8). Conspicuously often we find topaz crystals in the melt inclusions. Previously such crystals were discussed as chance co-trapping. However, a careful examination shows that the topaz is exclusively connected to the melt inclusions, no topaz crystals are trapped in the host quartz. Further examination shows that the amount of topaz is closely related to the water concentration of the corresponding melt inclusions. If we assume a fluorine content of 20% of the topaz, we obtain two separable but superimposed Gaussian distributions of fluorine versus the water content (Fig. 9). The two distributions can be traced back to changes in the F-speciation.

On the left side fluorine is the main diffusing species and near the critical point alkali-F-complexes, indicated by daughter minerals like elpasolite $[K_2NaAlF_6]$ and cryolithionite $[Na_3Li_3Al_2F_{12}]$. And further to the H_2O -rich side F-rich mica become the dominant daughter mineral. The Gaussian distribution of F versus H_2O is a strong argument against a trapping of minute topaz crystals by chance, which would never give such distribution.

Discussion. For the understanding of the processes, we propose the following scenario. We take a water-rich silicate melt patch of about

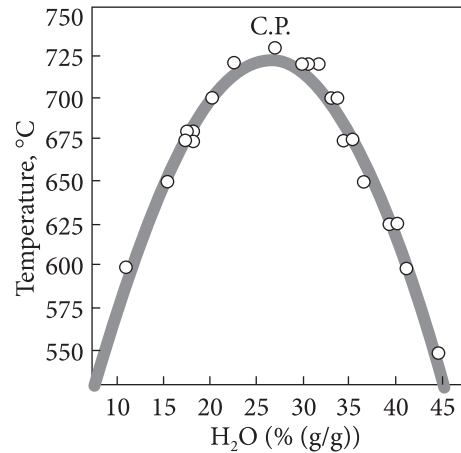


Fig. 8. The pseudo-binary solvus curve for the Volyn pegmatites. The critical point (C.P.) of the system: 732 °C, and 27.4% (g/g) H_2O

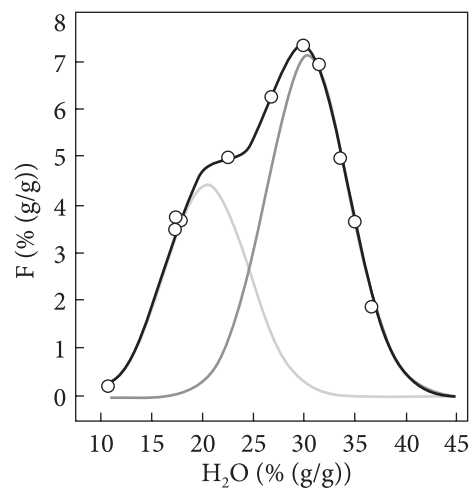


Fig. 9. Distribution of fluorine vs. the water concentration of some melt inclusions in pegmatite quartz from Volyn shows two separable but superimposed Gaussian distributions of fluorine versus the water content

10 m³ located in the roof-portion of the evolved Ehrenfriedersdorf tin-tungsten granite [29] and follow the changes in the patch with gradually cooling. At the start, we have a water concentration in the melt of about 20%. With differential cooling the crystallization of mostly water-free minerals like feldspars and quartz starts, which crystallize on the wall. Thus, the water content of the remaining melt increases significantly, possibly up to 30%, or a little more, by doing so it reaches supercritical or near supercritical conditions.

That such conditions are not rare events, can be seen also from Table, demonstrating that in the near-critical region of the pseudo-secondary

solvus there are an extremely strong element enrichments, which show Gaussian or Lorentzian distribution.

The Ehrenfriedersdorf pegmatite gives a very instructive example for the Be-enrichment in melt inclusions in quartz trapped immediately at the critical region of the solvus. The "current bulk" Be-content of these granites is about 15 ppm [4]. If we take the offset value of 284 ppm Be (Table) for the pegmatite, then the pegmatite melt is enriched by a factor of about 18.9 in Be. The highest analytically determined value at near-critical conditions that we have found is 11.810 ppm Be in some melt inclusions [25]. That means a further enrichment by about 41.6, or a total enrichment by a factor of ~790. Co-trapping of beryl crystals can be ruled out since the Be concentration shows a Gaussian distribution, co-trapping would show a purely random distribution, and should on occasions show beryl crystals in some inclusions pre-homogenization, none of which have been observed.

Such extreme enrichments demand an explanation and is conceivable only by irreversible processes of a previously undescribed nature. Table shows that in melt inclusions trapped in growing quartz near the critical point the element enrichment is a good approximation to Gaussian or Lorentzian distribution. However, according to new results, the distributions represent only a first approximation smoothed curves because extreme values are also possible. Currently the highest measured Be concentration in the above-mentioned Ehrenfriedersdorf case, is 71,490 ppm Be for melt inclusions trapped near-critical conditions. At such a value, the well-defined Lorentzian or Gaussian distribution degenerates into a single point. That means the Gaussian or Lorentzian curves near the critical point transition in two branches of exponential curves with different sign, where the concentration axis is an asymptote for both branches. That means further that theoretically the viscosity comes close to zero and the diffusivity goes towards infinity. This observation cast new light to the problem. The Gaussian and Lorentzian element distribution curves in the critical range are the first approximations, because exactly at the critical point the enrichment goes to extremely high values. Strictly speaking, the element enrichment/depletion near the critical point follow

an exponential increase, coming from the left side, and an exponential decrease going from the critical point to the right side. The phase in immediate vicinity to the critical point is neither a melt nor a fluid — we call this the supercritical state, which is mathematically and physically not exactly defined, however, has dramatic influence on the behaviour of the phases involved.

Because in the immediately vicinity of the critical point there are dramatic changes in the physical state there is also a significant change in the molecular structure, connected with an abrupt change in the speciation, which we can see based on different daughter minerals in melt inclusions in quartz trapped to the left or right to the critical point.

Under what conditions is such evolution possible?

In the Königshain granite, we have seen the side-by-side millimetre to centimetre thick vertical tracks decorated with water-rich melt inclusions. The water concentration of these inclusions is between 15 and 20% ([17] and therefore far from the equilibrium concentration of the surrounding granite with about 5% H₂O. We interpret these channels as transport channels for the pegmatite forming fluids. The continuous influx of water-rich melts into the pegmatite miarole or chamber increases this volume up to equilibrium, determined mainly by the intrusion level of the hosting granite. As we know from the Volodarsk-Volynski chamber pegmatites in Ukraine, the volume of such pegmatites can reach values of more than 6000 m³ [7]. In small granites like Königshain the diameter of such pegmatites range from centimetre to decimetre. The appearance of the same inclusion types and the same enrichment style in very different large pegmatite bodies (decimetre vs. thousand times greater bodies) implies a general process.

In a more macroscopic sense, the driving force for the action of equilibrium and non-equilibrium processes is the crystallization of a vast amounts of water-free crystals like quartz and feldspar, at first as graphic granite and later as single crystals of feldspar and quartz by gradual cooling of a water-rich silicate melt. Given this process, crystallization increase the water concentration at the boundary layer up to critical- and supercritical concentrations. Due to the density contrast and the surface tension, super-

critical melt moves away and through the under-critical melt volume and acts as a very effective and selective extraction phase. The upstream movement and convections in such a chamber work like a separating funnel and very effectively concentrate incompatible elements into the mobile phase.

Such convection cells can work as long as the viscosity of the bulk melt is low enough and the convection is not too strongly challenged by the crystallization of water-free minerals (mainly quartz, feldspar). In the temperature range between 750 and 500 °C, the system "miarolitic cavity" is in a non-equilibrium state. Because at the start the conditions in such system are quite different, and the end state is approximately the same, we have here a type of equifinality — at least an open system — a combination of a set of equilibrium and non-equilibrium processes. By the combination of system-cooling and step-by-step crystallization in the cavity, the processes are oscillating between supercritical state and the standard melt/fluid state down to temperatures (500 °C) where the fluid (hydrothermal) state becomes dominant.

Such type of equifinality is only conceivable if the pegmatite-forming system represent an open system which tends towards a steady-state. Equifinality means that from quite different starting points the evolution goes to an approximately equal end state. Pegmatite melts with very different starting composition develop to pegmatites with roughly the same end state of the classic granitic pegmatites.

The interaction of processes between equilibrium and non-equilibrium conditions makes the understanding of the whole processes very complicated.

The extreme enrichment of elements which form the characteristic Gaussian or Lorentzian distributions, lead exactly at the critical point to a singularity in concentration.

Ion exchange processes far away from the critical point, show a more-or-less linear relationship between concentration and another variable (temperature, water concentration) and are near-equilibrium processes. However, near the critical point, the physical properties change dramatically: the viscosity goes to zero, the diffusivity goes to infinity. Diffusions processes in this region are non-equilibrium processes. Other

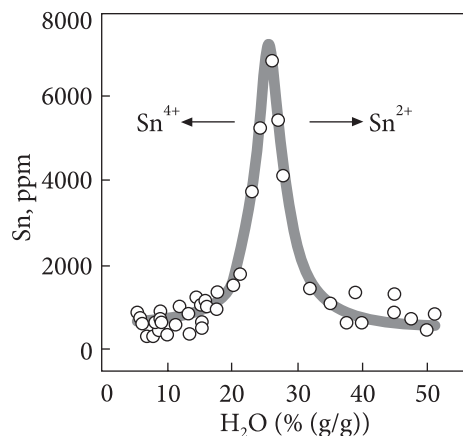


Fig. 10. Lorentz plot of the Sn concentration (in ppm) versus H₂O concentration for water-rich melt inclusions in pegmatite quartz from Ehrenfriedersdorf: Area 54207, centre 25.8% H₂O, width 5.2% H₂O, offset 547 ppm Sn, height 6606 ppm Sn. With cooling there is a change of the tin speciation: starting from the critical point in direction to the lower water concentration an increase of Sn⁴⁺, and in direction to higher water concentration the Sn²⁺ bearing species increase, indicated by the arrows

properties, also show such extreme changes: coefficient of thermal expansion, surface tension, heat capacity and others. That this region is something is very different to the surroundings has already been shown by Harrison and Mayer [3], see also further above. They postulated for the so-called "derby-hat" region an almost infinite compressibility [8, 10].

Generally, all processes in the near-critical region are non-equilibrium processes. A quantitative description is currently not possible.

The near-supercritical boundary layer between bulk melt and growing quartz crystal reacts as a surface-active zone, enabling the further enrichment of elements, and "organizes" a selective ion-exchange between the boundary layer and freshly trapped melt inclusions, which at the start is a homogeneous droplet of the boundary layer composition immediately trapped on the growing crystal. By forwarding growth of the host the inclusion is separated from the bulk boundary melt by a thin (but increasingly thick) semipermeable quartz membrane producing a electrophoretic potential. Since at near-critical conditions the viscosity goes to zero and the diffusivity goes towards infinity, we have a local extremely rapid ion exchange process producing the observed extreme element enrichments.

Note, however, that the boundary layer described has nothing to do with the "classic" boundary layer used for example by David London, although certain similarities are present. The main differences are the extremely low viscosity and the extreme mobility in the convection current. This extreme mobility leads also to a short-distance change in the element enrichment: the composition of adjoining (~ 10 to $50 \mu\text{m}$) inclusions can vary in wide limits — tin-rich side-by-side to tungsten-rich melt inclusions, or Beborates (berborite $[\text{Be}_2(\text{BO}_3)(\text{OH})\cdot\text{H}_2\text{O}]$) and Be-phosphates (beryllonite $[\text{NaBePO}_4]$). A very similar observation of extreme heterogeneity in element concentrations in inclusions only a few μm apart was noted in [5]. However, a different mechanism was proposed.

What we observe on microscopically small melt inclusions trapped in the critical region is valid also for a more macroscopic state in the pegmatitic cavity from cubic decimetre to hundreds of cubic meters.

From the results on two examples of different large pegmatite systems (Volyn chamber pegmatites vs. smaller miarolitic pegmatites), we see a selective enrichment of some ions in the water-rich melt inclusions formed under near-critical conditions in quartz of pre-pegmatitic and pegmatitic origin (Table). From this enrichment, we can deduce some preliminary conclusions.

According to our state of knowledge, this enrichment can be described well with Gaussian and/or Lorentzian functions with the characteristics: area, centre, width, offset, and height. The position of the maximum coincides (within experimental error) near the critical point of the pseudo-binary solvus. The height of the Gaussian and Lorentzian curves depends on the availability of the extractable elements near the growing crystal interface (a type of boundary layer), their mobility, and their speciation. Because the enrichment processes occur at the critical point and in their immediate neighbourhood, they are aspects of the irreversible thermodynamic impervious. That is not easy to understand, and there are a lot of open questions. Between the formation of the inclusions (trapping of a melt droplet on the growing surface and successive enclosing into the growing matrix) and complete trapping, the general "association" of processes is an open one, and also time-dependent.

The "supercritical region" around the critical point is a general of the curve surrounding of the solvus crest being very flat, generated by small fluctuations in temperature, pressure, and water concentration.

The element enrichment around the critical point generally differs from the classical, often simple linear element enrichment processes in geochemistry. The fundamental processes here are determined by the diffusion-determined selective ion transport in the supercritical state, which is also temperature, pressure, and concentration-dependent and enclose driving forces with linear and non-linear characters. The selectivity of the element enrichment raises essential questions: which processes are responsible for the selectivity and the directed flux? Diffusion alone cannot explain the overall process — diffusion is only one component. There are processes necessary that relate to entropy production [6]. The diffusion process alone is very complicated because the diffusion is a counter current diffusion (e.g., $\text{Be} \leftrightarrow \text{Na}$) through the growing thickness of the membrane layer (growing inclusion wall by the increase of the length between inclusion and crystal surface). The membrane's increasing thickness may be responsible for the Gaussian curve form of the element distribution versus water concentration.

In the primary inclusion system, there are alkali ions, the dominant species. Together with water, they are also responsible for maintaining the local supercritical state down to lower temperatures by deposition the system SiO_2 on the inclusion wall, which increases the alkali and water concentration relatively in the partial inclusion system.

A mathematical description of the processes is, for us up to now, not possible. All acting forces and fluxes are connected to unknown boundary conditions. We hope that our findings can serve as a basis for more theoretical considerations.

Conclusion. We have presented some examples of the extreme enrichment of different elements near the solvus crest of a pseudo-binary melt-water system. According to our observation this state is the consequence of the crystallization of water-rich silicate melts in a quasi-closed system such as miarolitic cavities. However, we have also seen that such evolution is not

only connected to such pegmatite-forming systems. Similar evolution paths we observed also at the beginning of the formation of quartz veins, exemplified by [19]. Furthermore, we often see such characteristic inclusion parageneses in high-temperature mineralization of very different origins. Mostly such near-critical inclusion types are arranged in the root zone of crystals (quartz, topaz, beryl and others). Because in these crystal zones the inclusion number is very high, the optical resolution is often restricted and the probability of overlooking such inclusions is very large.

There is also another problem in the inclusion research. By the prevailing and dominance of well-formed fluid inclusions often these primary formations are simply ignored as untypical and not explainable inclusions. Or were explained they are assumed to be formed by heterogeneous trapping and similar processes. Given such a philosophy only one part of the crystal-grow history is accepted. An instructive example is the emerald formation in the famous Habachtal deposit [21], where up to the work of [21] melt in-

clusions were not discussed or even recognised. Another example is the tin-tungsten mineralization in the Variscan Erzgebirge. The frequency distribution of the homogenization temperatures of fluid inclusions (see for example [12] suggests for the main formation of the tin-tungsten mineralization a temperature of $388 \pm 29^\circ\text{C}$ ($n = 1254$ measurements). From the work of [9] and the present work we know that tin-rich melt inclusions with homogenization temperatures around 700°C (see also Table) are very important for the tin budget in the Variscan tin-tungsten deposits of the Erzgebirge and elsewhere. Fig. 10 shows the Lorentzian distribution of Sn in melt inclusions in quartz from the Ehrenfriedersdorf pegmatite and the tendency of the change in speciation of Sn^{4+} vs. Sn^{2+} .

The same problems are generally present during the inclusion work on different minerals from classical pegmatites: overrating of fluid inclusions for the genesis and ignoring the often present melt inclusions.

Acknowledgment. We thank an anonymous reviewer for the remarks to improve the title and the text.

REFERENCES

1. Alimarin, I.P., Fadeeva, V.I. and Dorokhova, E.N. (1976), *Lecture experiments in analytical chemistry*, Mir Publ., Moscow, RU, 306 p.
2. Aranovich, L., Akinfiyev, N.N. and Golunova, M. (2020), *Chemical Geol.*, Vol. 550 (8), 119699. <https://doi.org/10.1016/j.chemgeo.2020.119699>
3. Harrison, S.F. and Mayer, J.E. (1938), *Journ. Chem. Phys.*, Vol. 6, pp. 101-104. <https://doi.org/10.1063/1.1750208>
4. Hösel, G. (1994), *Das Zinnerz-Lagerstättengebiet Ehrenfriedersdorf / Erzgebirge. Sächsisches Landesamt für Umwelt, Landwirtschaft und Geologie, Dresden*, Vol. 1, 195 p. <https://nbn-resolving.org/urn:nbn:de:bsz:14-qucosa-78881>
5. Kamenetsky, V.S., van Achterbergh, E., Ryan, C.G., Naumov, V.B., Mernagh, T.P. and Davidson, P. (2002), *Geology*, Vol. 30(5), pp. 459-462. [https://doi.org/10.1130/0091-7613\(2002\)030<0459:ECHOGD>2.0.CO;2](https://doi.org/10.1130/0091-7613(2002)030<0459:ECHOGD>2.0.CO;2)
6. Kammer, H.-W. and Schwabe, K. (1985), *Thermodynamik irreversibler Prozesse*, Weinheim, 114 p.
7. Pavlishin, V.I. and Dovgyi, S.A. (2007), *Mineralogy of the Volynian Champer Pegmatites, Ukraine*. Mineralogical Almanac, Vol. 12, 125 p.
8. Proctor, J.E. (2020), *The liquid and supercritical fluid states of matter*, CRC Press, 300 p.
9. Rickers, K., Thomas, R. and Heinrich, W. (2006), *Mineralium Deposita*, Vol. 41, pp. 229-245. <https://doi.org/10.1007/s00126-006-0057-7>
10. Sengers, J.L. (2002), *How fluids unmix*, Amsterdam, 302 p.
11. Sowerby, J.R. and Keppler, H. (2002), *Contrib. Mineral. Petrol.*, Vol. 143, pp. 32-37. <https://doi.org/10.1007/s00410-001-0334-5>
12. Thomas, R. (1982), *Ergebnisse der thermobarogeochemischen Untersuchungen an Flüssigkeitseinschlüssen in Mineralen der postmagmatischen Zinn-Wolfram-Mineralisation des Erzgebirges*, Freiburger Forschungshefte C370, 85 p.
13. Thomas, R. and Davidson, P. (2010), *Mineral. and Petrol.*, Vol. 100, pp. 227-239. <https://doi.org/10.1007/s00710-010-0132-8>
14. Thomas, R. and Davidson, P. (2012), *Ore Geol. Rews*, Vol. 46, pp. 32-46. <https://doi.org/10.1016/j.oregeorev.2012.02.006>
15. Thomas, R. and Davidson, P. (2013), *Journ. Geosci.*, Vol. 58, pp. 183-200. <https://doi.org/10.3190/jgeosci.135>
16. Thomas, R. and Davidson, P. (2015), *Lithos*, Vol. 212-215, pp. 462-468. <https://doi.org/10.1016/j.lithos.2014.08.028>

17. Thomas, R. and Davidson, P. (2016), *Lithos*, Vol. 260, pp. 225-241. <https://doi.org/10.1016/j.lithos.2016.05.015>
18. Thomas, R. and Davidson, P. (2016b), *Ore Geol. Revs.*, Vol. 72, pp. 1088-1101. <https://doi.org/10.1016/j.oregeorev.2015.10.004>
19. Thomas, R., Davidson, P. and Appel, K. (2019), *Acta Geochim.*, Vol. 38, pp. 335-349. <https://doi.org/10.1007/s11631-019-00319-z>
20. Thomas, R., Davidson, P. and Beurlen, H. (2012), *Mineral. and Petrol.*, Vol. 106, pp. 55-73. <https://doi.org/10.1007/s00710-012-0212-z>
21. Thomas, R., Davidson, P. and Rericha, A. (2020), *Mineral. and Petrol.*, Vol. 114, pp. 161-173. <https://doi.org/10.1007/s00710-020-00700-4>
22. Thomas, R., Davidson, P., Rericha, A. and Tietz, O. (2019), *Eine außergewöhnliche Einschlussparagenese im Quarz von Steinigtwolmsdorf / Oberlausitz*, Berichte der Naturforschenden Gesellschaft der Oberlausitz, Band 27, pp. 161-172.
23. Thomas, R., Förster, H.-J. and Heinrich, W. (2003), *Contrib. Mineral. Petrol.*, Vol. 144, pp. 457-472. <https://doi.org/10.1007/s00410-002-0410-5>
24. Thomas, R., Webster, J.D. and Davidson, P. (2006), Understanding pegmatite formation: The melt and fluid inclusion approach. Chapter 9 in Webster (ed.): Melt Inclusions in Plutonic Rocks, Short Course Series of the Mineralogical Association of Canada, Vol. 36, Montreal, pp. 189-210.
25. Thomas, R., Webster, J.D. and Davidson, P. (2011), *Contrib. Mineral. Petrol.*, Vol. 161, pp. 483-495. <https://doi.org/10.1007/s00410-010-0544-9>
26. Thomas, R., Webster, J.D. and Heinrich, W. (2000), *Contrib. Mineral. Petrol.*, Vol. 139, pp. 394-401. <https://doi.org/10.1007/s004100000120>
27. Veksler, I.V. and Thomas, R. (2002), *Contrib. Mineral. Petrol.*, Vol. 143, pp. 673-683. <https://doi.org/10.1007/s00410-002-0368-3>
28. Voznyak, D.K. (2007), *Microinclusion and reconstruction of conditions of endogenous mineral formation*, Nauk. dumka, Kyiv, UA, 280 p. [in Ukrainian].
29. Webster, J.D., Thomas, R., Rhede, D., Förster, H.-J. and Seltmann, R. (1997), *Geochim. et Cosmochim. Acta*, Vol. 61, Iss. 13, pp. 2589-2604. [https://doi.org/10.1016/s0016-7037\(97\)00123-3](https://doi.org/10.1016/s0016-7037(97)00123-3)

Received 01.11.2021

Райнер Томас, д-р наук (мінералогія)

Центр Гельмгольца Потсдам, Німецький дослідницький центр геонауки
Телеграфенберг, D-14473 Потсдам, Німеччина

E-mail: RainerThomas@t-online.de; <https://orcid.org/0000-0002-7699-7009>

Пол Девідсон, д-р наук

Університет Тасманії, CODES, Центр рудних родовищ і наук про Землю
Хобарт 7001, Австралія

E-mail: Paul.Davidson@utas.edu.au; <https://orcid.org/0000-0002-6129-0748>

Адольф Реріха, PhD. Алеманненштрасс, 4а, D-14612 Фалькензее Німеччина

E-mail: ruth.rericha@gmx.de; ScopusID 6504676937

Дмитро К. Возняк, д-р геол. наук

Інститут геохімії, мінералогії та рудоутворення ім. М.П. Семененка НАН України
03142, м. Київ, Україна, пр-т Акад. Палладіна, 34

E-mail: dkvoznayak@ukr.net; <https://orcid.org/0000-0002-6124-2033>

БАГАТІ ВОДОЮ РОЗПЛАВНІ ВКЛЮЧЕННЯ, ЯК ЗАГАРТОВАНІ ЗРАЗКИ НАДКРИТИЧНОГО СТАНУ В ГРАНІТАХ І ПЕГМАТИТАХ, ЩО ЕКСТРЕМАЛЬНО ЗБАГАЧЕНІ ЕЛЕМЕНТАМИ ЗА НЕРІВНОВАЖНИХ УМОВ

Показано, що в міаролітових пегматитах під час кристалізації багатих водою розплавів зразки цих мінералоутворювальних розплавів захоплено у вигляді багатих водою розплавних включень, які збереглися переважно в кварці. Об'ємна концентрація води і температура є системовизначальними параметрами, оскільки з їхнього аналізу випливає, що ці розплавні включення зображують псевдобінарні криві сольвуса в координатах температури та концентрації води. Окрім того, за допомогою зменшених координат (H_2O/H_2O_{crit} проти T/T_{crit}) більшість розплавних включень досліджуваних пегматитів дуже добре відображають у стандартизованій та зменшеній кривій сольвуса. Існування та утворення таких однорідних кривих розчину є вираженням процесів кристалізації у майже рівноважних умовах. Однак багато домішок і деякі основні елементи розплавних включень, захоплених біля гребеня сольвуса (H_2O/H_2O_{crit} від 0,5 до 1,5 і $T/T_{crit} > 0,95$), показують незвичайні розподіли з дуже добре визначеними кривими Гауса та/або Лоренца, що харак-

теризуються певною площею, центром, шириною, зміщенням та висотою. Це показано на багатьох природних прикладах, отриманих з пегматитів. Лише значення зміщення представляють умови, близькі до рівноваги та відповідні концентрації елементів, які еквівалентні регіональному числу Кларка (число Кларка — це відносна кількість хімічного елемента, як правило, у земній корі). Ми інтерпретуємо ці розподіли як пояснення деяких надзвичайних фізико-хімічних властивостей у цій критичній області: переважно надвисокою швидкістю дифузії, низькою динамічною в'язкістю та надзвичайно низьким поверхневим натягом. Поблизу критичної точки ми маємо й нерівноважні, й рівноважні процеси, пов'язані з простором і часом. Окрім того, ми можемо показати, що гаусовий і лоренцевий розподіл є першими наближеннями розподілу конкретних елементів, оскільки в критичній точці збагачення деяких елементів досягає такої міри, що гаусова та/або лоренцева криві вироджуються у вертикальну лінію (є асимптотичною до осі концентрації), що визначається максимальною розчинністю речовини в надкритичній системі розплав — вода. Найбільша концентрація Be, наприклад, спостерігалась у розплавних включеннях Еренфрідерсдорфа — 71490 ppm Be.

Ключові слова: пегматити, багаті H₂O розплавні включення, надкритичний стан, екстремальне збагачення елементами, розподіл Гауса/Лоренца.